LAWRENCE
LIVERMORE
NATIONAL
LABORATORY

UCRL-CONF-225959

Long Term Electrochemical Behavior of Creviced and Non-Creviced Alloy 22 in CaCl2 + Ca(NO3)2 Brines at 155°C

M. A. Rodríguez, M. L. Stuart, R. B. Rebak

November 9, 2006

Corrosion/2007 Conference and Exposition
Nashville, TN, United States
March 11, 2007 through March 15, 2007

Paper 07577 prepared for presentation to the Conference and Exposition Corrosion/2007 organized by NACE International in Nashville, TN, 11-15 March 2007

LONG TERM ELECTROCHEMICAL BEHAVIOR OF CREVICED AND NON-CREVICED ALLOY 22 IN $CaCl_2$ + $Ca(NO_3)_2$ BRINES AT 155°C

Martín A. Rodríguez, Marshall L. Stuart and Raul B. Rebak
Argentinean Commission of Atomic Energy, Buenos Aires, Argentina
Lawrence Livermore National Laboratory, Livermore, CA, 94550, USA

ABSTRACT

Alloy 22 is a nickel base alloy highly resistant to all forms of corrosion. In very aggressive conditions (*e.g.* hot concentrated chloride containing brines) Alloy 22 could suffer localized attack, namely pitting and crevice corrosion. Chloride ion is known to be the most detrimental aggressive agent for Alloy 22 and is able to promote crevice corrosion when tight crevices exist in hot chloride containing solutions of different concentrations. Nitrate ion is an effective inhibitor of chloride induced crevice corrosion when present in a high enough $[NO_3^-]/[Cl^-]$ ratio. The occurrence of localized corrosion in a given environment is governed by the values of the critical potential (E_{crit}) for crevice corrosion and the corrosion potential (E_{corr}) that the alloy may establish in the studied environment. If E_{corr} is equal or higher than E_{crit}, localized corrosion may be expected.

This paper discusses the evolution of E_{corr} and corrosion rate (CR) of Alloy 22 specimens in 18 m $CaCl_2$ + 9 m $Ca(NO_3)_2$ and 18 m $CaCl_2$ + 0.9 m $Ca(NO_3)_2$ brines at 155°C. Two types of specimens were used, polished as-welded (ASW) creviced and non-creviced specimens and as-welded plus solution heat-treated (ASW+SHT) creviced specimens. The latter contained the black annealing oxide film on the surface. Results show that, in a few immersion days E_{corr} reached a stable value higher than the open circuit potential of a platinum electrode in 18 m $CaCl_2$ + 9 m $Ca(NO_3)_2$ for all specimens tested. Specimens tested in this solution did not suffer any type of localized attack. On the other hand, E_{corr} showed oscillations of up to 600 mV in 18 m $CaCl_2$ + 0.9 m $Ca(NO_3)_2$ during the entire immersion period. These oscillations were due to pitting corrosion development. Crevice corrosion was not observed in any testing case. Corrosion rates for specimens in the latter solution ($[NO_3^-]/[Cl^-]$ = 0.05) were one order of magnitude higher than for specimens in the second one ($[NO_3^-]/[Cl^-]$ = 0.5). Nitrate showed to be able to inhibit localized attack even in hot concentrated chloride brines when present in a ratio of $[NO_3^-]/[Cl^-]$ = 0.5. Localized corrosion occurred only in condition where $E_{corr} > E_{crit}$.

Keywords: N06022, corrosion potential, corrosion rate, chloride, nitrate

INTRODUCTION

Alloy 22 (N06022) is a nickel (Ni) based alloy that contains nominally 22% chromium (Cr), 13% molybdenum (Mo), 3% tungsten (W) and 3% iron (Fe) (ASTM B 575). [1] Alloy 22 is able to remain passive in most industrial environments because of its high level of Cr, and therefore has an exceptionally low general corrosion rate. [2-4] The presence of Cr, Mo and W in balanced concentrations imparts Alloy 22 with high resistance to localized corrosion such as pitting corrosion, crevice corrosion and stress corrosion cracking even in hot high chloride (Cl^-) solutions. [5-10] It has been reported that Alloy 22 may suffer crevice corrosion when tightly creviced specimens are anodically polarized in chloride containing solutions. [6-8,11-13] It is also known that the presence of nitrate (NO_3^-) and other oxyanions in the solution minimizes or eliminates the susceptibility of Alloy 22 to crevice corrosion. [6-8,14-23] An important parameter is the ratio ($[NO_3^-]/[Cl^-]$) which has a strong effect on the susceptibility of Alloy 22 to crevice corrosion. [14-20] The higher the nitrate to chloride ratio, the stronger the inhibition by nitrate.

From the general and localized corrosion point of view, it is important to know the value of E_{corr} for Alloy 22 under different environmental conditions. [16] The corrosion degradation model for the Yucca Mountain nuclear waste container assumes that localized corrosion will only occur when E_{corr} is equal or greater than a critical potential (E_{crit}). [16] This is a necessary but not sufficient condition. That is, in environments that may promote crevice corrosion, if $E_{corr} < E_{crit}$ or $\Delta E = E_{crit} - E_{corr} > 0$, general or passive corrosion will occur and localized corrosion is not expected. In environments that promote localized corrosion, E_{crit} is the lowest potential that would initiate a localized attack. The value of E_{crit} is generally ascribed as the repassivation potential for crevice corrosion obtained using the cyclic potentiodynamic polarization (CPP) curve described in ASTM G 61. [16] From the CPP, the repassivation potential may be taken as the potential at which the reverse scan line crosses over the forward scan. This potential is called the repassivation potential cross over (ERCO). The repassivation potential could also be taken as ER1 or the potential for which the current density in the reverse scan reaches 1 $\mu A/cm^2$. [13] In short, by knowing the values of E_{corr} and E_{crit} (ER1) of Alloy 22, the likelihood or necessary conditions for the alloy to suffer crevice corrosion under natural polarization (e.g. oxygen from air) can be established.

Dunn et al. reported that the values of E_{corr} of Alloy 22 in air saturated 4 M Cl^- solution at 95°C were in the range between –300 and –100 mV SCE (-260 to –60 mV SSC). [12] Similarly, the E_{corr} of Alloy 22 in 0.028 M Cl^- pH ~ 10 at 95°C was reported to be between –200 and 0 mV SCE (-160 to +40 mV SSC). [12] Dunn et al. also stated that low temperature air oxidized specimens produced more scattered values of E_{corr} than did polished specimens. [12] In pH 2.7 solution of 0.028 M NaCl at 95°C the stabilized E_{corr} was approximately +250 mV SCE (+290 mV SSC). [12] That is, a lower pH promoted a stronger passivation thus resulting in a higher value of E_{corr}. Similar findings were reported by Estill et al. who reported that in acidic multi-ionic solutions simulating concentrated ground water the E_{corr} of Alloy 22 could be as high as +400 mV SSC at 90°C. [24] However, in pH 10 multi-ionic solutions the steady state E_{corr} was below +100 mV SSC. [24] The increase in the value of E_{corr} is generally accompanied by a decrease in the value of corrosion rate. [7,25] For example, it was reported that when Alloy 22 was immersed in aerated simulated acidified water (SAW) at 90°C, the E_{corr} increased from approximately –300 mV to +300 mV SSC in one week. [7] At the same time, the corrosion rate dropped one order of magnitude, from approximately 1 μm/year after immersion to approximately 0.1 μm/yr after one week exposure. [7] Similarly, creviced Alloy 22 specimens immersed in aerated NaCl + KNO_3 brines at 100°C had corrosion rates in the order of 30 nm/yr after 250 days full immersion.

The purpose of the current work was to monitor the behavior of E_{corr} and corrosion rate for welded Alloy 22 creviced specimens in 18 m $CaCl_2$ + 9 m $Ca(NO_3)_2$ and 18 m $CaCl_2$ + 0.9 m $Ca(NO_3)_2$ brines at 155°C for about 600 days. The specimens (creviced and non-creviced) were tested both in the

as-welded (ASW) condition and also in the as-welded plus solution heat-treated condition (ASW+SHT). The latter specimens contained the black annealing oxide film on the surface.

EXPERIMENTAL TECHNIQUE

Alloy 22 (N06022) specimens used to assess corrosion potential (E_{corr}) and corrosion rate (CR) as a function of immersion time were machined from welded 1.25-inch thick plates (~32 mm). Table 1 shows the chemical composition of the heats for the base plate and the welding wire. The plates were welded using the gas tungsten arc welding (GTAW) technique from both sides of the plate using the double V groove technique. The specimens were in the form of prism crevice assemblies (PCA) (Figure 1). The dimensions of the PCA were: 0.375 inch thick, 0.75 inch high and 0.75 inch wide. The exposed surface area of each specimen was 14.06 cm². This surface area did not include the area covered by the crevice formers, which was approximately 1.5 cm². The PCA had a mounting mechanism for the connecting rod explained in ASTM G 5 (Figure 1). [26] All the specimens had a weld seam through the center of the cross section. The crevice formers were mounted on both sides of the specimen (Figure 1). Each crevice former consisted of a washer made of a ceramic material containing 12 crevicing spots or teeth with gaps in between the teeth (ASTM G 48). [26] The width of the weld seam was not the same for both faces where the crevice formers (CF) were mounted, that is, in some instances the teeth of the CF were resting solely on weld material and in others on a weld and wrought mix of material. Before mounting them onto the metallic specimens, the CF were covered with PTFE military grade tape to ensure a tight crevicing gap. The specimens had a ground surface finish of 600-grit paper. There are two types of PCA specimens in this work: (1) The as-welded (ASW) which were as-received welded specimens and (2) the as-welded plus solution heat treated (ASW + SHT) which were annealed in air for 20 min at 1121°C and then water quenched. The latter specimens were finished with 600-grit paper before the heat treatment but the final oxide formed as a consequence of annealing and water quenching was not disturbed prior to testing. The ASW + SHT specimens were black with slight tones of green, typical of high temperature formed chromium oxide. All the test specimens were fully immersed in the test solution. For each surface and metallurgical condition (ASW and ASW + SHT) there were four PCA specimens of Alloy 22 in each Cell 35 and 36 or in each electrolyte. Each cell also contained two welded ¼-inch diameter rods of Alloy 22. The rods were machined from welded plates, similarly as the PCA specimens described above. The end of the rods that contained the weld seam was partially immersed in the respective electrolytes. The rods were freshly finished with paper 600. The E_{corr} of all ten Alloy 22 specimens were monitored continuously.

In all the environments, the E_{corr} of pure platinum rods (ASTM B 561) [1] was also monitored. The platinum rods were 1/8-inch in diameter and 12-inch long. The Pt rods were immersed 1-inch deep into the electrolyte solutions.

Table 2 shows the composition of the two test solutions expressed in molality (*m*), which represents moles of the salt per kilogram of the solvent (water). The solutions were prepared using calcium chloride ($CaCl_2$), calcium nitrate ($CaNO_3$) and de-ionized water. The salts were completely soluble at the tested conditions. At ambient temperature the solutions are mostly solid. The volume of the electrolyte solution in each cell was 2 liters (2 L). The testing temperature was 155°C. The electrolyte solutions were naturally aerated; that is, the solutions were not purged, but a stream of air was circulated above the level of the solution. This stream of air exited the vessel through a condenser to avoid evaporation of the electrolyte.

The E_{corr} was monitored using saturated silver chloride electrodes [SSC] through a Luggin capillary. The reference electrode was kept at room temperature using a jacketed electrode holder through which cooled water was re-circulated. The bridge in the reference electrode was filled with 5 M $CaCl_2$ solution to keep it liquid at ambient temperatures. The potentials in this paper are reported in the satu-

rated silver chloride scale [SSC or Ag/AgCl]. At ambient temperature, the SSC scale is 199 mV more positive than the normal hydrogen electrode (NHE).

The value of the free corrosion potentials or open circuit potentials were acquired using a commercial data acquisition (DA) unit that had the input resistance set at 10 G-ohm. Typically, the measurements were acquired every minute for the first day and every hour after the first day. The data was logged into in the internal memory of the DA unit and simultaneously to a spreadsheet in an interfaced personal computer. Usually, data back up was performed monthly.

At the same time that E_{corr} was being monitored for all ten Alloy 22 specimens, the polarization resistance (PR) of three specimens was also monitored as a function of time using the ASTM G 59 technique. [26] Testing of the polarization resistance do not affect the value of the corrosion potential since the polarization is minimal around the value of the rest potential. Polarization resistance measurements were performed in one ASW rod, one ASW PCA and one ASW + SHT PCA specimen in each cell (marked as PR in Table 3). The resistance to polarization was generally measured at 24 h of the first immersion, at 7 days, at 28 days and at every four weeks after that. The polarization resistance values ($\Omega.cm^2$) were later converted to corrosion rates (μm/year). To measure the polarization resistance, an initial potential of 20 mV below the corrosion potential (E_{corr}) was ramped to a final potential of 20 mV above E_{corr} at a rate of 0.167 mV/s. Linear fits were constrained to the potential range of 10 mV below E_{corr} to 10 mV above E_{corr}. In a plot potential vs. current the slope is defined as R_p or resistance to polarization (ASTM G 59). To calculate R_p, the potential was plotted in the X-axis and the current (dependent variable) in the Y-axis. The Tafel constants, b_a and b_c, were assumed to be $\pm$ 0.12 V/decade. It is known that if a metal is passive, the value of anodic portion of the Tafel constant could be much larger than that of the cathodic portion. However, the objective of this paper was to monitor the effect of immersion time keeping all other variables the same. That's the reason the Tafel constants were assumed constant for all the tested condition and for both portions of the polarization curve. The values of the Tafel constants should actually be determined separately for each tested condition but this task was beyond the objective of the paper. Corrosion rates were calculated using Equations 1 and 2

$$i_{corr} = \frac{1}{R_p} \times \frac{b_a \cdot b_c}{2.303(b_a + b_c)} \qquad (1)$$

$$CR(\mu m / yr) = k \frac{i_{corr}}{\rho} EW \qquad (2)$$

Where k is a conversion factor (3.27×10^6 $\mu m \cdot g \cdot A^{-1} \cdot cm^{-1} \cdot yr^{-1}$), i_{corr} is the corrosion current density in A/cm^2, which is calculated from resistance to polarization (R_p) slopes, EW is the equivalent weight of Alloy 22 (23.28 g), and ρ is the density of Alloy 22 (8.69 g/cm^3). The EW was calculated assuming an equivalent dissolution of the major alloying elements as Ni^{2+}, Cr^{3+}, Mo^{6+}, Fe^{2+}, and W^{6+} (ASTM G 102). [26]

The start and finish dates for each cell are given in Table 3. At the finish date, a cyclic potentiodynamic polarization (CPP) was performed on the same specimens that were used for polarization resistance tests (Table 3). Then the specimens were removed from the cells, disassembled and then were examined under 20X magnification for evidence of localized corrosion. At the time of the preparation of the manuscript, the solution composition at the end of the tests was not measured to determine if decomposition of some of the species occurred or the concentration of corroded species.

EXPERIMENTAL RESULTS AND DISCUSSION

Evolution of the Corrosion Potential of Alloy 22

Table 3 lists the final value of E_{corr} of Alloy 22 and platinum specimens in the two electrolyte solutions (Cells 35 and 36). The final E_{corr} is the average of the last 30 consecutive immersion days. The corresponding standard deviation is also shown. The exposure times for the specimens were 602 days for those in Cell 35 and 588 days for those in Cell 36 (Table 3). All tests were terminated on 25-Apr-06.

Figures 2-6 show the evolution of the E_{corr} of platinum and Alloy 22 specimens as a function of the immersion time in Cells 35 and 36. Platinum is considered an inert electrode in many environments and therefore the value of E_{corr} of platinum is a measure of the redox potential of the system. All the acquired data was plotted in Figures 2 and 3 for all the tested specimens. For clarity, only the data for one of each Alloy 22 specimen type (ASW and ASW + SHT) is shown in Figures 4 and 5.

Figures 2 and 4 show the values of E_{corr} as a function of time in 18 m $CaCl_2$ + 9 m $Ca(NO_3)_2$ brine at 155ºC (Cell 35). The E_{corr} of Pt was stable as a function of time at approximately 500 mV. The E_{corr} of all Alloy 22 specimens was stable and higher than E_{corr} of Pt electrode during the entire test (Figures 2 and 4). The final value of E_{corr} of all Alloy 22 specimens was between 500 and 600 mV and its standard deviation during the last 30 immersion days was small (Table 3). E_{corr} seemed to have reached a steady state value for each of the specimens. The final E_{corr} values were slightly higher for creviced ASW+SHT specimens than for creviced ASW specimens (Table 3). Also, the standard deviation of the ASW + SHT specimens was higher than for the ASW specimens. The final E_{corr} value of the non-creviced rods was the lowest of all the three type of specimens. The rods also had the highest standard deviation. It is possible that the higher standard deviation for the rods was an effect of the noise produced by the partial immersion of these specimens in the electrolyte.

Figures 3 and 5 show the values of E_{corr} as a function of time in 18 m $CaCl_2$ + 0.9 m $Ca(NO_3)_2$ brine at 155ºC (Cell 36). The E_{corr} of Pt was stable as a function of time at about 500 mV. The E_{corr} of all Alloy 22 specimens showed oscillations of several hundreds of mV (up to 500 mV) during the entire test (Figures 3 and 5). Rod specimens showed lower E_{corr} values than PCA specimens during the last 30 immersion days (Table 3). Standard deviations for all the Alloy 22 specimens were about 100 mV (Table 3), much higher than for the specimens in Cell 35.

Detailed oscillations of E_{corr} between day 400 and day 450 are shown in Figure 6 for Pt and one of each type of Alloy 22 specimen (ASW Rod and creviced ASW and ASW + SHT) immersed in Cell 36. The E_{corr} of Pt remained constant during the period shown. On the other hand, E_{corr} values of Alloy 22 specimens showed continuous oscillations from noble near-Pt potential values to potentials below 100 mV (Figures 6). Amplitude of oscillation seemed to be higher for ASW Rod and ASW PCA specimens than for ASW+SHT PCA specimen. A more detailed observation (not shown) indicated that the oscillation period was about 1 day for each one of the specimens. However, a higher oscillation frequency (lower oscillation period) cannot be discarded as the data acquisition frequency was about 4 times a day (every 8 hours) for this immersion time.

A different evolution of E_{corr} in time was found as $Ca(NO_3)_2$ concentration reduced from 9 m (Cell 35) to 0.9 m (Cell 36), the other conditions remaining the same (18 m $CaCl_2$ base brine at 155ºC). A stable E_{corr} value higher than E_{corr} of Pt electrode was found for all Alloy 22 specimens immersed in Cell 35. On the other hand, an oscillating E_{corr} value was found for all Alloy 22 specimens immersed in Cell 36. Visual examination of the specimens after immersion indicated that all Alloy 22 specimens in Cell 35 were free of pitting and crevice corrosion. Pitting corrosion attack was detected in the specimens tested in Cell 36. It may be assumed that the fluctuations in the E_{corr} of the specimens in Cell 36 could be associated to nucleation and further repassivation of localized corrosion (*i.e.* pitting and/or

crevice corrosion). When localized corrosion is initiated the E_{corr} drops which causes the localized corrosion to repassivate which in turn causes the E_{corr} to increase again, repeating the cycle.

In general, for Cell 35, the average E_{corr} values of the ASW + SHT specimens were higher and/or increased more rapidly than those of the ASW specimens. For Cell 36 (Table 3) the average E_{corr} value for the ASW + SHT specimens was slightly lower than for the ASW specimens.

The Corrosion Rate of Alloy 22

Figures 7 and 8 show corrosion rate (CR) of Alloy 22 specimens (one of each type of Alloy 22 specimen) as a function of immersion time for Cells 35 and 36. The corrosion potential at the time of each measurement is also shown in Figures 7-8. The corrosion rate for specimens in Cell 35 did not show dependence with E_{corr}. While the E_{corr} slightly decreased as time increased, the CR remained approximately constant (Figure 7). The ASW+SHT PCA specimen showed the lowest corrosion rates, in the range of 0.2-0.3 μm/yr throughout the entire immersion period (Figure 7). The ASW PCA and ASW Rod specimens showed similar corrosion rates, which varied slightly in time (from 0.2 to 3 μm/yr). The measured corrosion rates are low values taking into account the extreme experimental conditions such of high temperature and high chloride concentration of the brine. The brine in Cell 35 has an approximate concentration of 77% (salt mass per mass of solution).

The corrosion rate and E_{corr} for the specimens in Cell 36 showed important fluctuations in time (Figure 8). E_{corr} fluctuations made it hard to perform polarization resistance measurements as E_{corr} was not stable during the measurement and shifted when the specimen was polarized. The measured CR values ranged from 0.1 to 30 μm/yr. The ASW+SHT PCA specimen also showed the lowest corrosion rate values in Cell 36. CR for the ASW + SHT specimen decreased as E_{corr} increased (Figure 8). Oscillations in E_{corr} and CR for the ASW PCA and ASW Rod specimens can be roughly correlated. In general, an increase in corrosion rate is associated with a potential drop (Figure 8). This is particularly observed for the ASW Rod. It could be related to nucleation and further repassivation of localized corrosion. When localized attack occurs, the shown CR value in Figure 8 is only indicative of the event. The actual CR in the localized area may be higher but non-measurable using polarization resistance technique.

The ASW+SHT PCA specimens showed low corrosion rates in the both studied solutions and did not suffer observable pitting corrosion after the test in Cell 36. This could be related with the presence of the black annealing oxide scale. The CR for ASW PCA and ASW Rods were higher in Cell 36 than in Cell 35. These latter specimens suffered pitting corrosion in the free exposed area in Cell 36. They only suffered uniform transpassive dissolution in Cell 35. The oxide films formed on the specimens were not analyzed after the tests.

The corrosion rates reported here are for comparative purposes only, for example, to compare the effect of time on the corrosion rate or the effect of electrolyte solution. The corrosion rates reported here may not represent the actual values of the corrosion rates, which are more appropriately determined using weight-loss measurements (ASTM G 31 and G 1). [26]

Cyclic Potentiodynamic Polarization of Alloy 22

Figures 9 and 10 show the cyclic potentiodynamic polarization curves for Alloy 22 in the brines contained in Cells 35 and 36, respectively. The tests were performed after the approximately 600 days of immersion of the specimens in each cell (Table 3).

Figure 9 shows that both the creviced PCA specimen and the partially immersed rod behaved the same in this electrolyte. The breakdown potential E20 for both specimens was higher than 800 mV SSC (Table 4). This potential is well into the transpassive region of potentials for the dissolution of chro-

mium as chromate (+VI). For both specimens the reverse scan progressed without hysteresis, suggesting the absence of localized corrosion. The repassivation potential ER1 was high at approximately 600 mV (Table 4). None of the externally polarized specimens in Cell 35 suffered localized corrosion (Figure 9 and Table 4). They suffered transpassive dissolution due to the highly applied potentials of values higher than 1 V.

Figure 10 shows the anodic behavior of a creviced PCA and a partially immersed rod in the electrolyte in Cell 36. Even though the corrosion potential and the current density in the forward scan for the two specimens was different, the current density in the reverse scan for both specimens was the same. Table 4 shows that the repassivation potential ER1 was 8 mV SSC for the PCA specimen and 31 mV SSC for the rod specimen. Both specimens showed ample hysteresis in the reverse scan, suggesting the presence of localized corrosion. The fact that the ER1 was the same for both specimens shows that both specimens showed the same type of attack. Examination of the specimens after the tests showed that both of them had pitting corrosion. The pitting corrosion was likely present before the polarization experiments were conducted but were probably reactivated during the CPP test.

Figure 11 shows comparatively the cyclic polarization curves of the creviced PCA specimen in Cell 36 with a MCA creviced specimen in the same electrolyte but only after immersing for 24-hr in deaerated conditions. Figure 11 shows that the specimen immersed for 20 months in the aerated brine had a higher corrosion potential and a higher resistance to breakdown. However, once the localized corrosion was re-initiated, the reverse scan was the same for both specimens and the repassivation potential was also the same for both specimens (Tables 4 and 5).

Typical Potentials from the Cyclic Potentiodynamic Polarization Curves

Table 4 and Table 5 show the breakdown and repassivation potentials for welded Alloy 22 after 20 months in aerated brines and after short term deaerated tests. Results from both tables suggest that the repassivation potential is practically the same regardless of the immersion time. For example, in the Cell 35 type environment with a nitrate over chloride ratio of 0.5, the ER1 for Alloy 22 was higher than 600 mV SSC for both the deaerated and aerated electrolytes. None of the specimens suffered localized attack after the tests. Alloy 22 did not become more prone to attack after the 20 months immersion in the highly concentrated aerated brine at 160°C. In the Cell 36 type environment, the repassivation potential ER1 for the long term immersed specimens were 8 and 31 mV SSC (Table 4) and for the freshly immersed specimens in deaerated electrolytes were 11 and 7 mV (Table 5). For practical purposes these values are identical. Findings in Tables 4 and 5 show that the short term measurement of the repassivation potential in deaerated solutions represent also the values of repassivation potential under aerated conditions and after long-term immersion.

Values of characteristic potentials from Table 4 show that the specimens containing the black annealed oxide film were slightly more resistant to localized attack than the specimens with a freshly polished surface.

Figure 12 shows the comparison between the repassivation potentials ER1 (Table 5) [21] and the values of E_{corr} for rods after long term immersion in the aerated electrolytes (Table 3). The short term tests to determine characteristic repassivation potentials were conducted at 160°C; however the long term tests in aerated solutions for E_{corr} were at 1500°C. For Cell 35, which had a nitrate over chloride ratio of 0.5, ER1 was higher than E_{corr}. Localized corrosion was not expected and did not occur. For Cell 36, which had a nitrate over chloride ratio of 0.05, ER1 was lower than E_{corr} (Figure 12). For this type of environment (Cell 36), localized corrosion might be expected and occurred.

Observation of Specimens After 20 Months in the Aerated Electrolytes

Table 6 shows the description of the 12 specimens after the tests for Cells 35 and 36. In each cell, three specimens were polarized at the end of the exposure time.

All the specimens immersed in Cell 35 were free from localized corrosion, even after the cyclic polarization of the three selected specimens. Figure 13 shows transpassivity in the bold surfaces of the ASW PCA, which was freshly polished before the tests. The footprints of the crevice formers are clearly visible and they are free from crevice corrosion under them. The extent or depth of the transpassive corrosion in the freely exposed surfaces has not been measured yet. The ASW rods were also free from localized corrosion. The ASW + SHT (black annealed) specimens had less evident corrosion than the freshly polished specimens (Figure 14). A complete assessment of the attack is not possible without a metallographic sectioning.

The non black annealed specimens immersed for 20 months in the electrolyte in Cell 36 suffered pitting corrosion. The resulting electrolyte solution was yellow at the end of the test. Figure 15 shows the ASW PCA (freshly polished) after the tests. Attack was in the form of pitting corrosion in the bold surfaces. The area under the crevice formers was free from attack. The attack in the bold surfaces was extended, and was especially severe in the weld seam (not shown). Also, in the short transverse direction, the attack seemed to follow lamination or rolling direction features. This is not an unusual observation for Alloy 22, since it suffers similar attack in other environments (for example wet HF). Each one of the ASW rod specimens suffered one large corrosion pit near the water line location. The rest of the immersed specimen was free from corrosion. The corrosion site was fully covered by a highly glassy appearance black oxide. This is oxide is known to be rich in chromium and especially in molybdenum and tungsten. The black oxide site was also surrounded by white and greenish salt-like deposits. Away from the corrosion spot and deeper into the solution it is obvious that some dissolved metal (not analyzed yet) precipitated back onto the specimen forming fern-like structures on the surface of the specimen. The ASW + SHT specimens suffered little obvious dissolution (Figure 16). A metallographic sectioning is still needed to confirm that there is no attack under the surface black oxide film.

Concluding Remarks

It has been reported that localized corrosion can occur in Alloy 22 whenever the E_{corr} is equal or greater than the repassivation potential in the tested conditions. That is, if $\Delta E = ER1 - E_{corr} \geq 0$, localized corrosion will not occur. This is a necessary but not sufficient condition. Current results confirm this rule of localized corrosion predictability. Current results show that even though the corrosion potential of Alloy 22 could be highly anodic (such as in Cell 35), localized corrosion is not going to occur because of other conditions in the system. In Cell 35, even though E_{corr} is in the order of 500 mV SSC (Table 3 and Figure 12), the specimens were free from localized corrosion because ER1 was even higher. Moreover, in Cell 35 the nitrate over chloride ratio was 0.5 (Table 2), which may have been enough in those conditions to inhibit the initiation and propagation of localized corrosion. On the other hand, in Cell 36, localized corrosion occurred because $\Delta E < 0$ (Figure 12) and because the nitrate over chloride ratio was only 0.05 (Table 2), which was not enough to inhibit localized corrosion. Thus, current tests confirm that the inhibitive effect of nitrate for localized corrosion is active even in highly concentrated brines (36 molal chloride) and at high temperature (160°C).

Current results also confirm that repassivation potentials measured using cyclic potentiodynamic polarization in short term tests in deaerated solutions actually represent the repassivation potential values of Alloy 22 for longer immersion times and under aerated conditions.

CONCLUSIONS

1. Alloy 22 immersed in highly concentrated 18 m $CaCl_2$ + $Ca(NO_3)_2$ brines at 155°C showed high corrosion potentials (E_{corr}).
2. For a nitrate over chloride ratio of 0.5 (Cell 35), the E_{corr} was stable and in the range of + 500 mV SSC.
3. For a nitrate over chloride ratio of 0.05 (Cell 36), E_{corr} showed oscillations of near 500 mV
4. All the specimens immersed in Cell 35 were free from localized corrosion after 20 months immersion in the aerated electrolytes. The polished specimens showed transpassive general dissolution
5. All the freshly polished specimens immersed in Cell 36 showed signs of localized corrosion (pitting corrosion)
6. The occurrence or absence of localized corrosion in the specimens could be inferred by the continuous monitoring of the open circuit potential and the polarization resistance R_p
7. Specimens with large variations in R_p (corrosion rate) or open circuit potential as a function of time showed localized corrosion after the tests
8. The presence of the black annealed film on the specimens seemed to be beneficial (offered additional protection) under the tested conditions

ACKNOWLEDGMENTS

Sharon G. Torres and her group are acknowledged for performing the solution heat treatments of the specimens. This work was performed under the auspices of the U. S. Department of Energy by the University of California Lawrence Livermore National Laboratory under contract N° W-7405-Eng-48. This work is supported by the Yucca Mountain Project, which is part of the DOE Office of Civilian Radioactive Waste Management (OCRWM).

REFERENCES

1. ASTM International, Volume 02.04, Standard B 575 (ASTM International, 2003: West Conshohocken, PA).
2. Haynes International, “Hastelloy C-22 Alloy”, Brochure H-2019E (Haynes International, 1997: Kokomo, IN).
3. R. B. Rebak in Corrosion and Environmental Degradation, Volume II, p. 69, Wiley-VCH, Weinheim, Germany (2000).
4. R. B. Rebak and P. Crook “Influence of the Environment on the General Corrosion Rate of Alloy 22,” PVP-Vol 483 pp. 131-136 (ASME, 2004: New York, NY).
5. R. B. Rebak and P. Crook “Improved Pitting and Crevice Corrosion Resistance of Nickel and Cobalt Based Alloys,” ECPV 98-17, pp. 289-302 (The Electrochemical Society, 1999: Pennington York, NJ).
6. B. A. Kehler, G. O. Ilevbare and J. R. Scully, Corrosion, 1042 (2001).

7. K. J. Evans and R. B. Rebak in Corrosion Science – A Retrospective and Current Status in Honor of Robert P. Frankenthal, PV 2002-13, p. 344-354 (The Electrochemical Society, 2002: Pennington, NJ).
8. K. J. Evans, S. D. Day, G. O. Ilevbare, M. T. Whalen, K. J. King, G. A. Hust, L. L. Wong, J. C. Estill and R. B. Rebak, PVP-Vol. 467, Transportation, Storage and Disposal of Radioactive Materials – 2003, p. 55 (ASME, 2003: New York, NY).
9. Y-M. Pan, D. S. Dunn and G. A. Cragnolino in Environmentally Assisted Cracking: Predictive Methods for Risk Assessment and Evaluation of Materials, Equipment and Structures, STP 1401, pp. 273-288 (West Conshohocken, PA: ASTM 2000).
10. R. B. Rebak in Environmentally Assisted Cracking: Predictive Methods for Risk Assessment and Evaluation of Materials, Equipment and Structures, STP 1401, pp. 289-300 (West Conshohocken, PA: ASTM 2000).
11. C. S. Brossia, L. Browning, D. S. Dunn, O. C. Moghissi, O. Pensado and L. Yang "Effect of Environment on the Corrosion of Waste Package and Drip Shield Materials," Publication of the Center for Nuclear Waste Regulatory Analyses (CNWRA 2001-03), September 2001.
12. D. S. Dunn, L. Yang, Y.-M. Pan and G. A. Cragnolino "Localized Corrosion Susceptibility of Alloy 22," Paper 03697 (NACE International, 2003: Houston, TX).
13. K. J. Evans, A. Yilmaz, S. D. Day, L. L. Wong, J. C. Estill and R. B. Rebak "Comparison of Electrochemical Methods to Determine Crevice Corrosion Repassivation Potential of Alloy 22 in Chloride Solutions," JOM, January 2005 (to be published).
14. G. A. Cragnolino, D. S. Dunn and Y.-M. Pan "Localized Corrosion Susceptibility of Alloy 22 as a Waste Package Container Material," Scientific Basis for Nuclear Waste Management XXV, Vol. 713 (Materials Research Society 2002: Warrendale, PA).
15. D. S. Dunn and C. S. Brossia "Assessment of Passive and Localized Corrosion Processes for Alloy 22 as a High-Level Nuclear Waste Container Material," Paper 02548 (NACE International, 2002: Houston, TX).
16. J. H. Lee, T. Summers and R. B. Rebak "A Performance Assessment Model for Localized Corrosion Susceptibility of Alloy 22 in Chloride Containing Brines for High Level Nuclear Waste Disposal Container," Paper 04692 (NACE International, 2004: Houston, TX).
17. G. O. Ilevbare, K. J. King, S. R. Gordon, H. A. Elayat, G. E. Gdowski and T. S. E. Gdowski, Journal of The Electrochemical Society, 152, 12, B547-B554, 2005
18. D. S. Dunn, L. Yang, C. Wu and G. A. Cragnolino, Material Research Society Symposium, Spring 2004, San Francisco, Proc. Vol 824 (MRS, 2004: Warrendale, PA)
19. D. S. Dunn, Y.-M. Pan, K. Chiang, L. Yang, G. A Cragnolino and X. He "Localized Corrosion Resistance and Mechanical Properties of Alloy 22 Waste Package Outer Containers" JOM, January 2005, pp 49-55.
20. R. B. Rebak, Paper 05610, Corrosion/2005 (NACE International, 2005: Houston, TX)
21. G. O. Ilevbare, R. A. Etien, J. C. Estill, G. A. Hust, A. Yilmaz, M. L. Stuart, and R. B. Rebak, "Anodic Behavior of Alloy 22 in High Nitrate Brines at Temperatures Higher than 100°C" by - Paper 93423 in the Proceedings of PVP2006-ICPVT-11, 2006 ASME Pressure Vessels and Piping Division Conference, July 23-27, 2006, Vancouver, BC, Canada
22. G. O. Ilevbare, Corrosion, 62, 340 (2006)
23. R. M. Carranza, M. A. Rodriguez and R. B. Rebak, "Inhibition of Chloride Induced Crevice Corrosion in Alloy 22 by Fluoride Ions," Paper 06622, Corrosion/2006, NACE International, March 12-16, 2006, San Diego, CA (NACE International, Houston, TX)
24. J. C. Estill, G. A. Hust and R. B. Rebak "Long Term Corrosion Potential Behavior of Alloy 22," Paper 03688 (NACE International, 2003: Houston, TX).

25. K. J. Evans, M. L. Stuart, R. A. Etien, G. A. Hust, J. C. Estill and R. B. Rebak, Corrosion/2006, Paper 06623 (NACE International, 2006: Houston, TX).
26. ASTM International, Volume 03.02, Standards G 1, G 5, G 31, G 48, G 59, G 61, G 102 (ASTM International, 2003: West Conshohocken, PA).

TABLE 1
CHEMICAL COMPOSITION OF THE TESTED SPECIMENS (Wt%)

Elements →	Ni	Cr	Mo	W	Fe	Others
Nominal ASTM B 575 N06022	50-62	20-22.5	12.5-14.5	2.5-3.5	2-6	2.5Co-0.5Mn-0.35V max
Welded Specimens Heats						
Base Metal Heat 2277-0-3183	55.29	21.23	13.37	2.93	3.65	1.7Co-0.23Mn-0.14V
Weld Wire Seam Heat XX1829BG	59.31	20.44	14.16	3.07	2.2	0.21Mn-0.15Cu

TABLE 2
COMPOSITION OF THE ELECTYROLYTE SOLUTIONS (m)

Cells ↓ / Species →	$[Cl^-]$ (m)	$[NO_3^-]$ (m)	$[Cl]/[NO_3^-]$	$[NO_3^-]/[Cl^-]$
35	18	9	2	0.5
36	18	0.9	20	0.05

TABLE 3
LIST OF CELL AND SPECIMENS FOR CORROSION POTENTIAL (E_{corr}) STUDIES

CELL 35: 18 m $CaCl_2$ + 9 m $Ca(NO_3)_2$ 155ºC $[NO_3^-]/[Cl^-]$ = 0.5 Starting Date: 31-AUG-04 - End Date: 25-APR-06 - 602 days in solution				
Specimen ID	Metall.Cond. / Specimen Type	E_{corr} Final	E_{corr} St.Dev.	Average
WEA030	Pt Wrought Rod	524	3	524
KE0268 (PR)	ASW PCA	533	5	
KE0269	ASW PCA	541	6	
KE0270	ASW PCA	540	6	
KE0271	ASW PCA	537	6	538
KE0238 (PR)	ASW SHT PCA	582	16	
KE0239	ASW SHT PCA	582	14	
KE0240	ASW SHT PCA	577	6	
KE0241	ASW SHT PCA	567	7	577
JE2078 (PR)	ASW Rod	519	42	
JE2079	ASW Rod	505	38	512

CELL 36: 18 m $CaCl_2$ + 0.9 m $Ca(NO_3)_2$ 155ºC $[NO_3^-]/[Cl^-]$ = 0.05 Starting Date: 14-SEP-04 - End Date: 25-APR-06 - 588 days in solution				
Specimen ID	Metall.Cond. / Specimen Type	E_{corr} Final	E_{corr} St.Dev.	Average
WEA024	Pt Wrought Rod	487	2	487
KE0272 (PR)	ASW PCA	449	93	
KE0273	ASW PCA	431	103	
KE0274	ASW PCA	464	70	
KE0275	ASW PCA	414	63	439
KE0242 (PR)	ASW SHT PCA	421	63	
KE0243	ASW SHT PCA	420	60	
KE0244	ASW SHT PCA	421	59	
KE0245	ASW SHT PCA	446	129	427
JE2080 (PR)	ASW Rod	129	38	
JE2081	ASW Rod	176	82	153

The Final E_{corr} is the average of the last 30 consecutive immersion days and E_{corr} St.Dev. is corresponding standard deviation in this period.

TABLE 4
CHARACTERISTIC POTENTIALS FROM CYCLIC POLARIZATION CURVES IN mV, SSC
ASW PCA SPECIMENS AFTER 602 (CELL 35) AND 588 (CELL 36) DAYS IN
$CaCl_2 + Ca(NO_3)_2$ AERATED ELECTROLYTES AT 155°C

Cell	Specimen	Cl^- (m)	NO_3^- (m)	Ave E_{corr} 20 Mo. [A]	Pre-Test E_{corr}	E20	E200	ER10	ER1	ERCO
35	ASW Rod JE2078	36	18	519	516	821	1038	639	581	577
35	ASW PCA KE0268	36	18	533	527	837	1059	764	662	873
35	ASW SHT PCA KE0238	36	18	582	573	1052	>1200	946	812	818
36	ASW Rod JE2080	36	1.8	129	114	185	563	16	8	NA
36	ASW PCA KE0272	36	1.8	449	141	547	690	35	31	NA
36	ASW SHT PCA KE0242	36	1.8	421	303	653	677	68	47	NA

A From Table 3. NA = The cross over occurred at potentials below E_{corr}
E20 and E200 are breakdown potentials or the potential in the forward scan of a CPP for which the current density reached 20 and 200 μA/cm². ER10 and ER1 are repassivation potentials or the potential in the reverse scan of a CPP for which the current density reached 10 and 1 μA/cm². ERCO is also a repassivation potential or the potential at which the reverse scan intersects the forward scan.

TABLE 5
CHARACTERISTIC POTENTIALS FROM POLARIZATION CURVES IN mV, SSC
FRESHLY POLISHED SPECIMENS AFTER 24-h IMMERSION IN
$CaCl_2 + Ca(NO_3)_2$ DEAERATED ELECTROLYTES AT 160°C (REF. 21)

Specimen ID	Type of Specimen	Solution	E20	E200	ER10	ER1	ERCO
JE3461	ASW MCA	18 m $CaCl_2$	-93	-40	-174	-185	-184
JE3462	ASW MCA	18 m $CaCl_2$	-134	-73	-77	-83	NA
JE3274	ASW MCA	18 m $CaCl_2$ + 0.9 m $Ca(NO_3)_2$	93	123	14	11	11
JE3282	ASW MCA	18 m $CaCl_2$ + 0.9 m $Ca(NO_3)_2$	71	108	7	7	NA
JE3280	ASW MCA	18 m $CaCl_2$ + 2.7 m $Ca(NO_3)_2$	208	307	209	173	235
JE3283	ASW MCA	18 m $CaCl_2$ + 2.7 m $Ca(NO_3)_2$	163	280	79	67	65
JE3275	ASW MCA	18 m $CaCl_2$ + 9 m $Ca(NO_3)_2$	NA	NA	NA	NA	NA
JE3281	ASW MCA	18 m $CaCl_2$ + 9 m $Ca(NO_3)_2$	862	NA	825	698	NA

NA = Not Available

TABLE 6
OBSERVATION FROM SPECIMENS EXPOSED 602 (CELL 35) AND 588 (CELL36) DAYS IN AERATED ELECTROLYTES AT 155°C

Cell	Specimens	$[Cl^-]$ (m)	$[NO_3^-]$ (m)	Observations
35	ASW PCA KE0268	18	9	No CC. Transpassive Dissolution. – CPP Performed
35	ASW PCA KE0269	18	9	No CC. Transpassive Dissolution
35	ASW PCA KE0270	18	9	No CC. Transpassive Dissolution
35	ASW PCA KE0271	18	9	No CC. Transpassive Dissolution
35	ASW SHT PCA KE0238	18	9	No CC – CPP Performed
35	ASW SHT PCA KE0239	18	9	No CC
35	ASW SHT PCA KE0240	18	9	No CC
35	ASW SHT PCA KE0241	18	9	No CC
35	ASW Rod JE2078	18	9	No PC – CPP Performed
35	ASW Rod JE2079	18	9	No PC
36	ASW PCA KE0272	18	0.9	Severe PC. Lamination attack. No CC. CPP Performed
36	ASW PCA KE0273	18	0.9	Severe PC. Lamination attack. No CC
36	ASW PCA KE0274	18	0.9	Severe PC. Lamination attack. No CC
36	ASW PCA KE0275	18	0.9	Severe PC. Lamination attack. No CC
36	ASW SHT PCA KE0242	18	0.9	Severe PC. No CC. CPP Performed
36	ASW SHT PCA KE0243	18	0.9	No apparent PC. No CC
36	ASW SHT PCA KE0244	18	0.9	No apparent PC. No CC
36	ASW SHT PCA KE0245	18	0.9	No apparent PC. No CC
36	ASW Rods JE2080	18	0.9	Thick green/black deposit at waterline. PC under deposit. No attack below waterline. – CPP Performed
36	ASW Rods JE2081	18	0.9	Thick green/black deposit at waterline. PC under deposit. No attack below waterline.

CC = Crevice Corrosion, PC = Pitting Corrosion, CPP = Cyclic Potentiodynamic Polarization
Lamination attack is a type of corrosion that seems to follow ghost lines in the lamination direction causing partial splitting of material layers. It is similar to the case of exfoliation corrosion commonly reported for aluminum alloys.

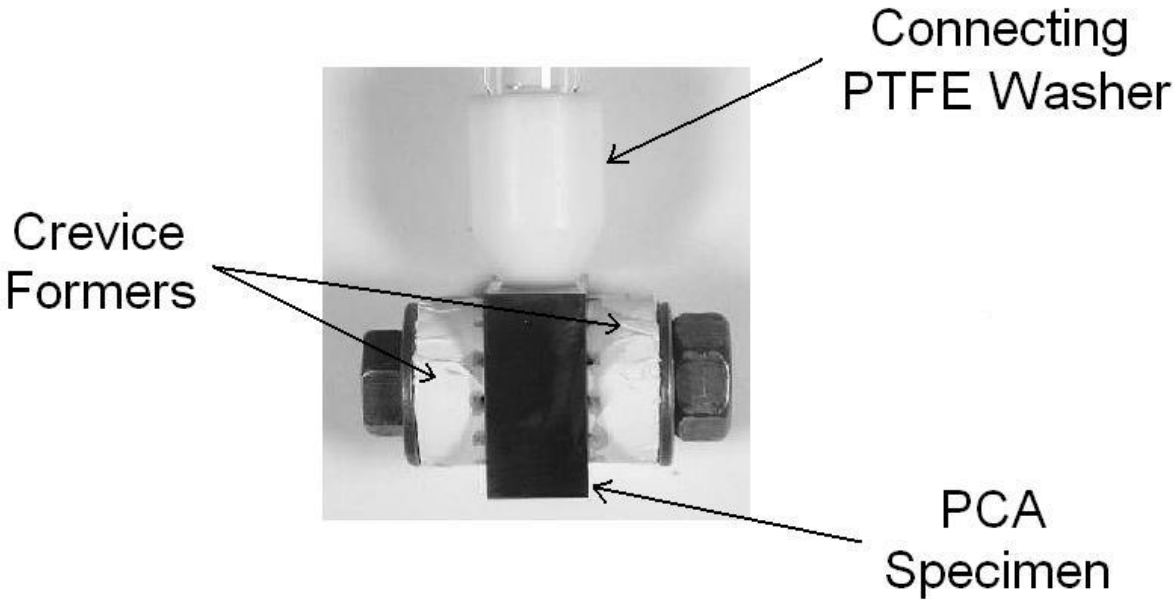

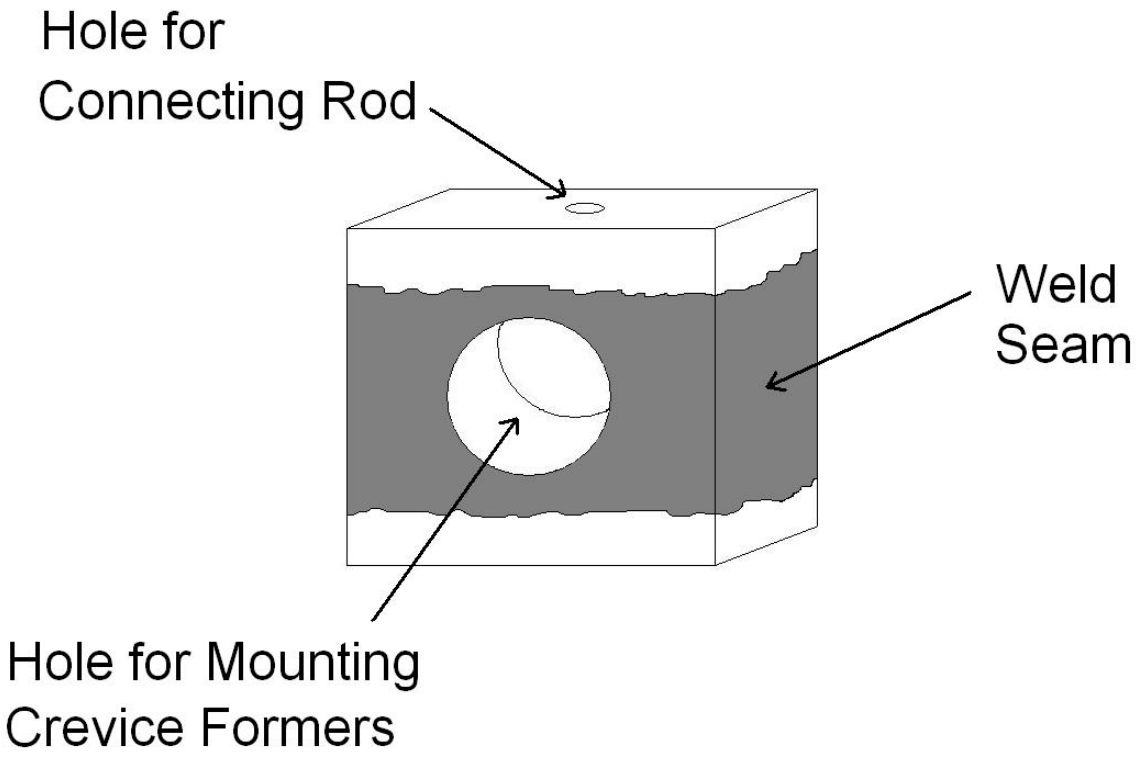

FIGURE 1 - PCA Specimen (0.75 x 0.75 x 0.375 inch or approx. 20 x 20 x 10 mm), The weld seam was not the same width on both faces of the specimen.

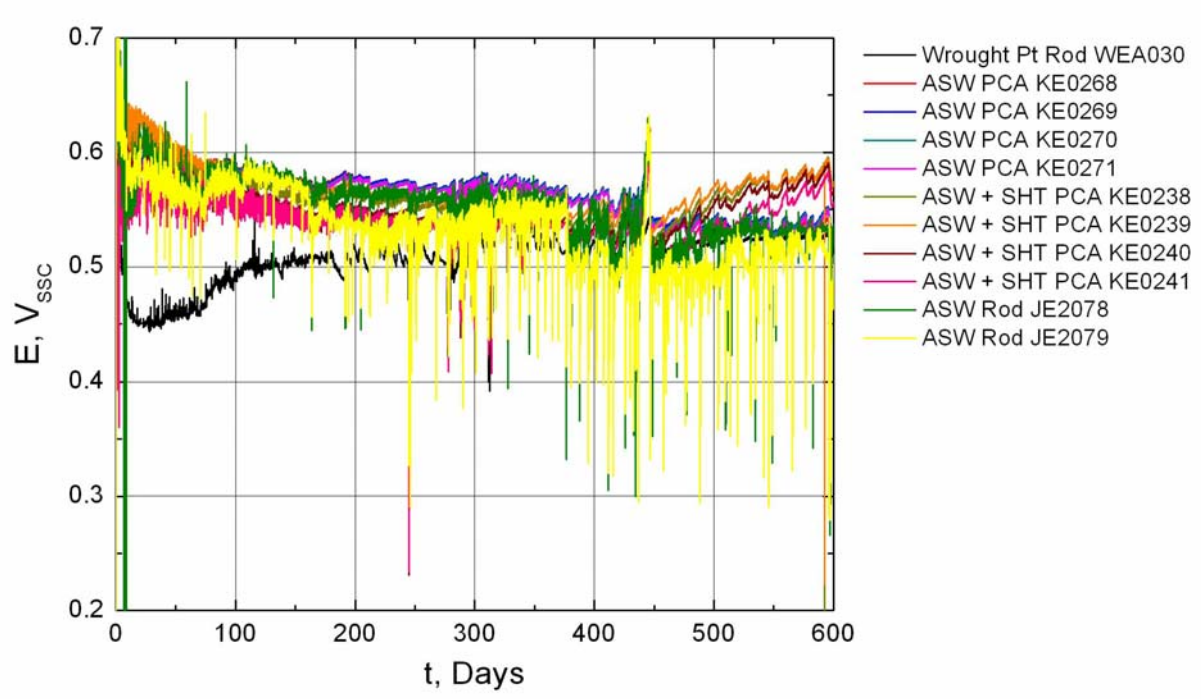

FIGURE 2 – Corrosion Potential (E_{corr}) as a function of immersion days for ASW and ASW+SHT Alloy 22 specimens immersed in Cell 35 (18 m $CaCl_2$ + 9 m $Ca(NO_3)_2$ at 155°C).

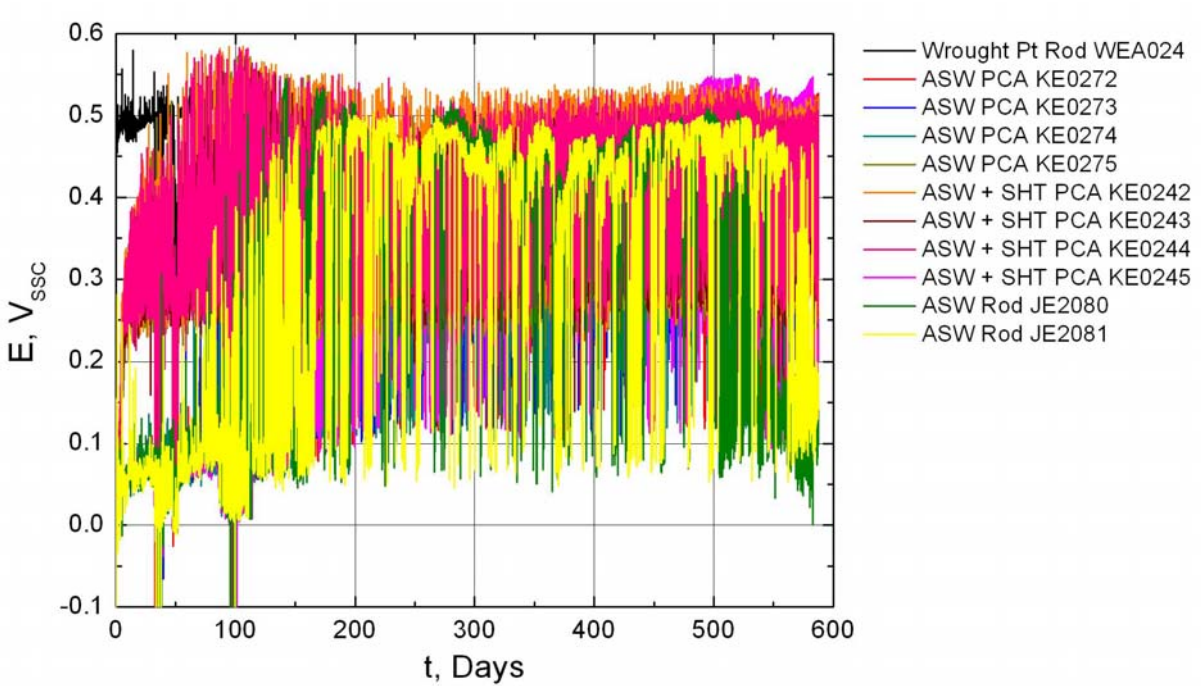

FIGURE 3 – Corrosion Potential (E_{corr}) as a function of immersion days for ASW and ASW+SHT Alloy 22 specimens immersed in Cell 36 (18 m $CaCl_2$ + 0.9 m $Ca(NO_3)_2$ at 155°C).

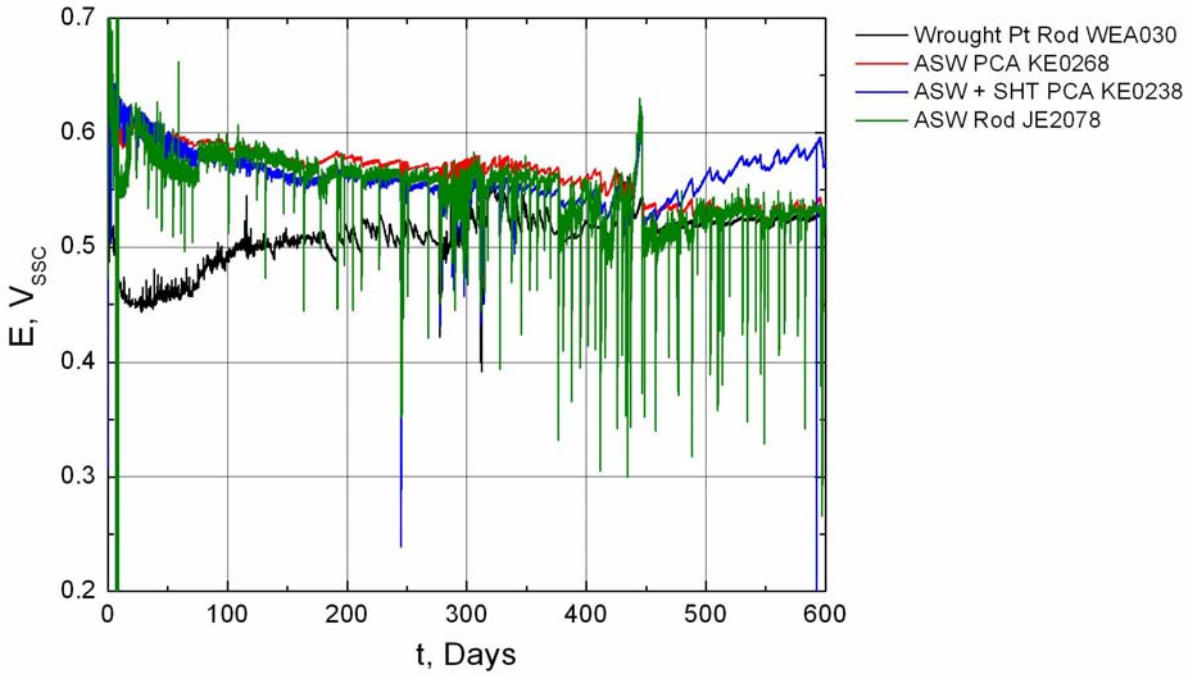

FIGURE 4 – Corrosion Potential (E_{corr}) as a function of immersion days for selected ASW and ASW+SHT Alloy 22 specimens immersed in Cell 35 (18 m $CaCl_2$ + 9 m $Ca(NO_3)_2$ at 155°C).

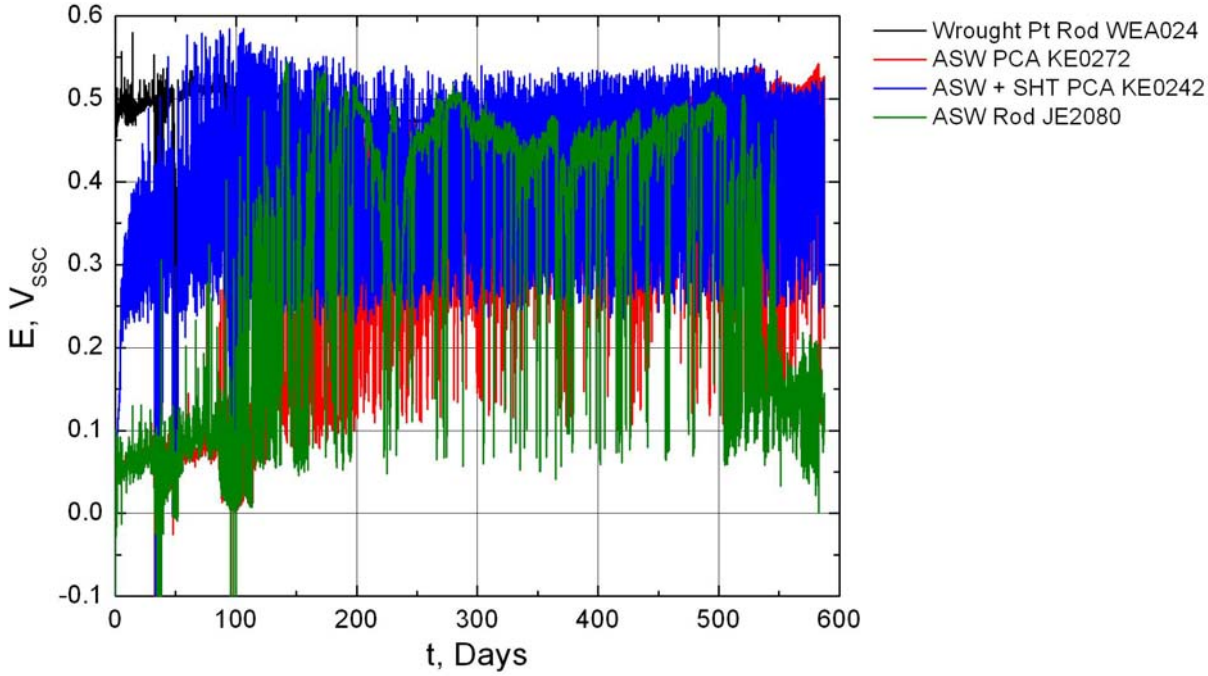

FIGURE 5 – Corrosion Potential (E_{corr}) as a function of immersion days for selected ASW and ASW+SHT Alloy 22 specimens immersed in Cell 36 (18 m $CaCl_2$ + 0.9 m $Ca(NO_3)_2$ at 155°C).

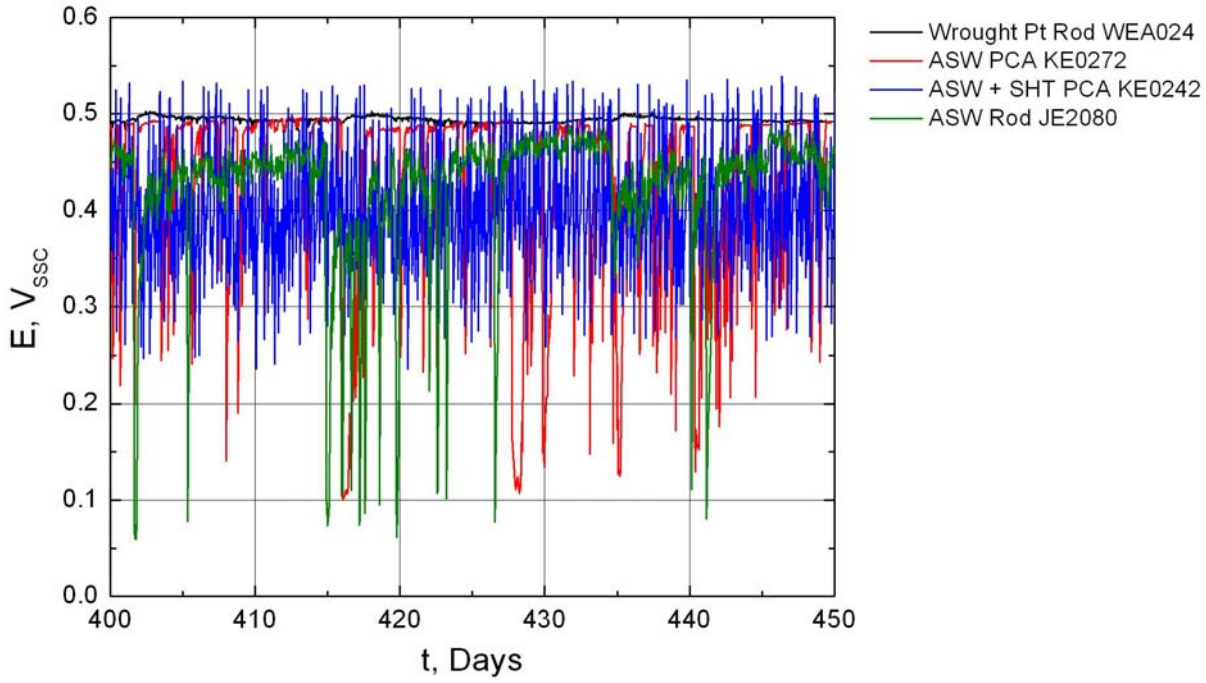

FIGURE 6 – Corrosion Potential (E_{corr}) as a function of immersion days for selected ASW and ASW+SHT Alloy 22 specimens immersed in Cell 36 (18 m $CaCl_2$ + 0.9 m $Ca(NO_3)_2$ at 155°C). Values between immersion day 400 and 450 are only shown.

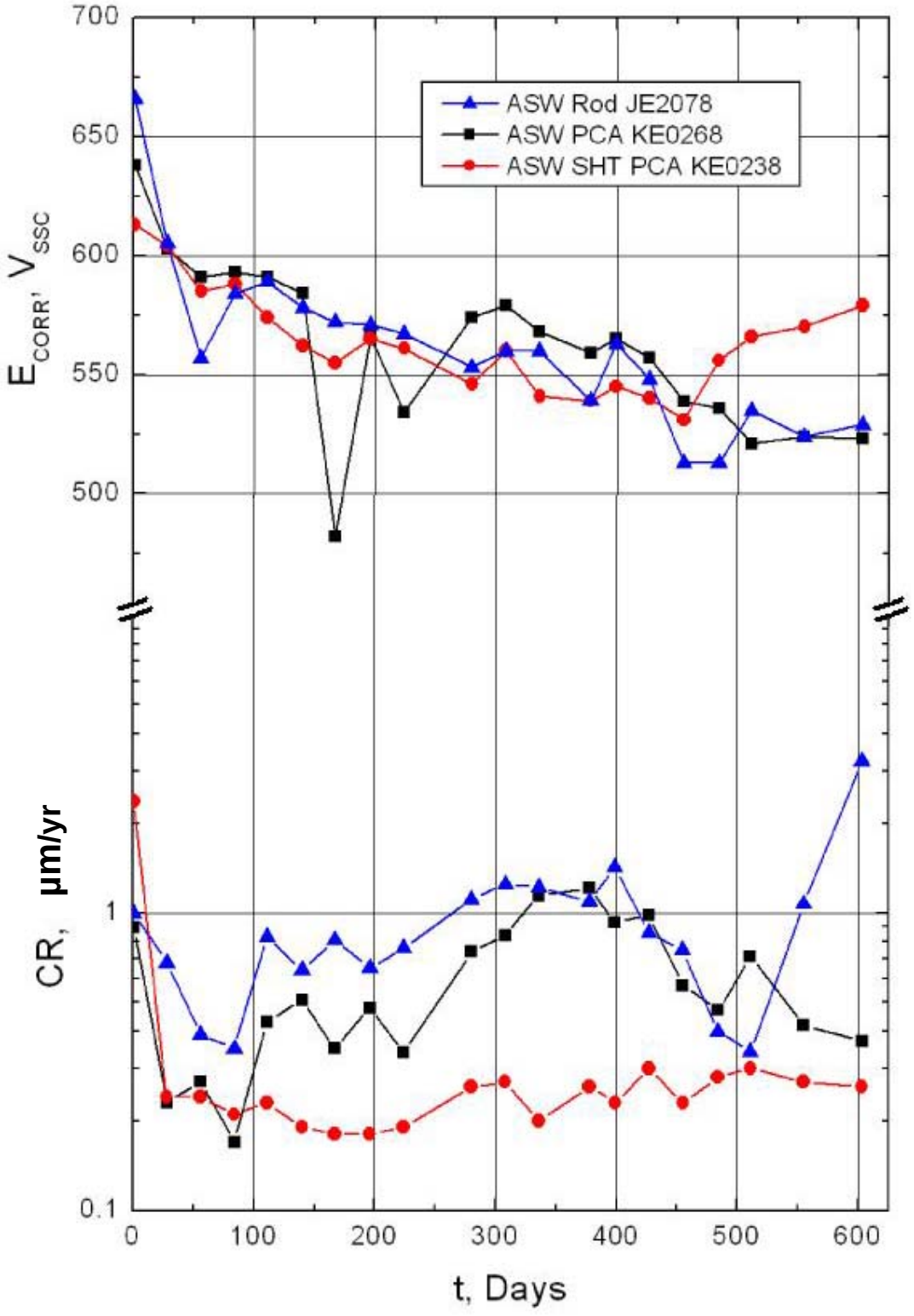

FIGURE 7 – Corrosion Potential (E_{corr}) and Corrosion Rate (CR) as a function of immersion days for selected Alloy 22 specimens immersed in Cell 35 (18 m $CaCl_2$ + 9 m $Ca(NO_3)_2$ at 155°C).

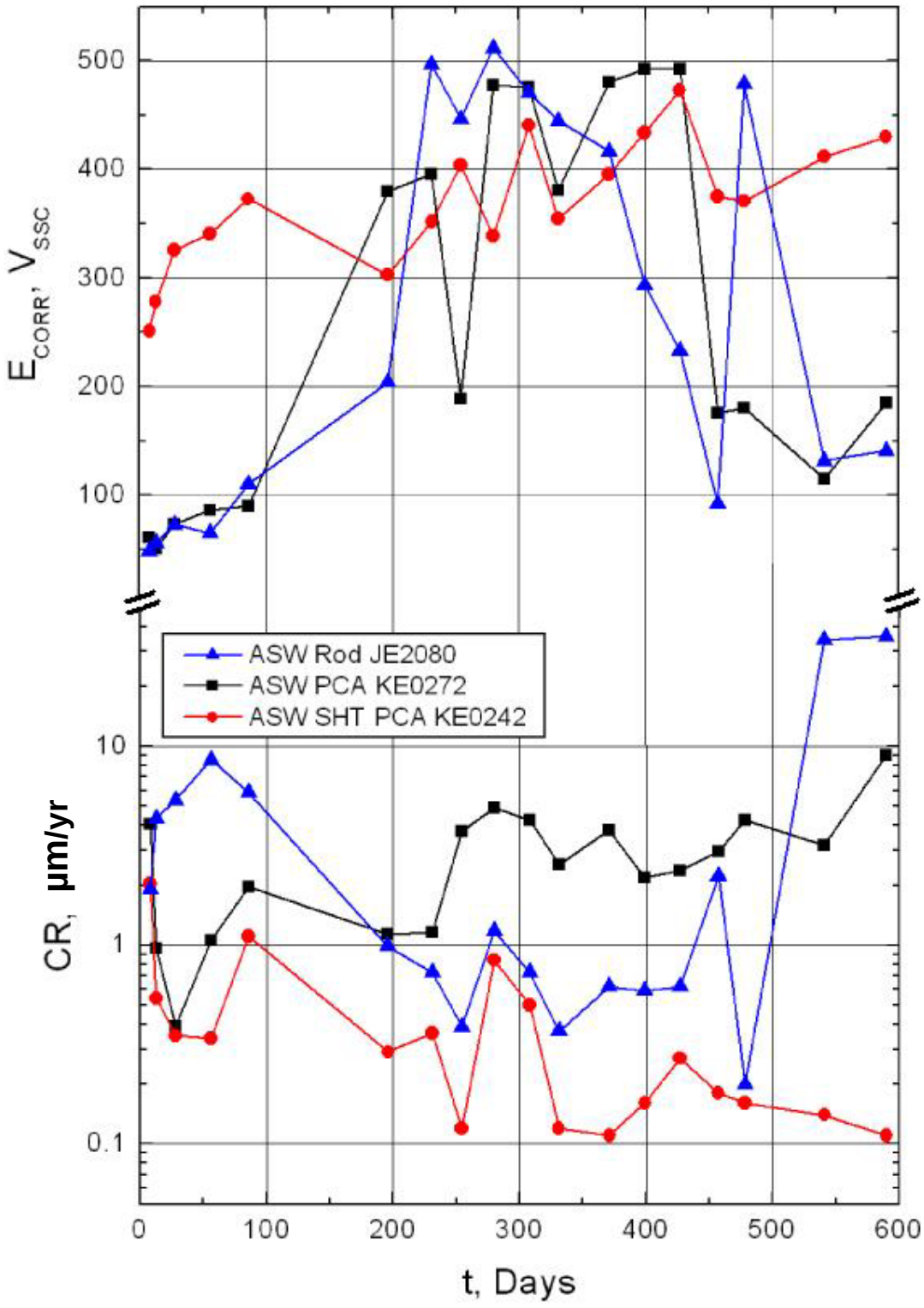

FIGURE 8 – Corrosion Potential (E_{corr}) and Corrosion Rate (CR) as a function of immersion days for selected Alloy 22 specimens immersed in Cell 36 (18 m $CaCl_2$ + 0.9 m $Ca(NO_3)_2$ at 155°C).

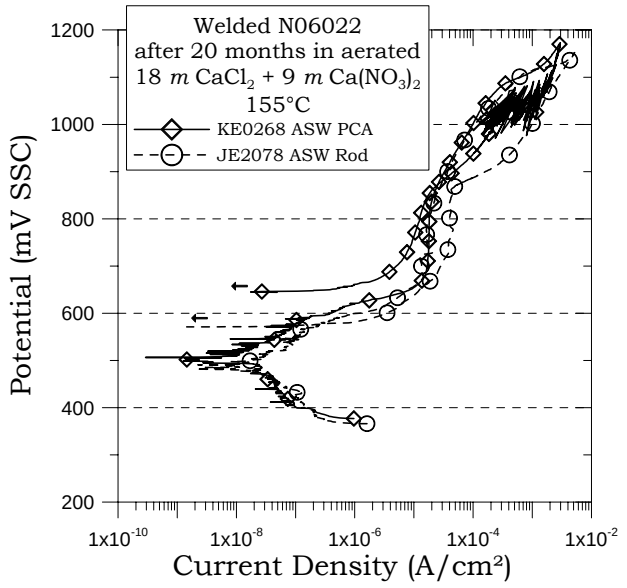

FIGURE 9 – Cyclic Potentiodynamic Polarization for Alloy 22 in 18 *m* $CaCl_2$ + 9 *m* $Ca(NO_3)_2$, $[NO_3^-]/[Cl^-]$ = 0.5 at 155°C (Cell 35)

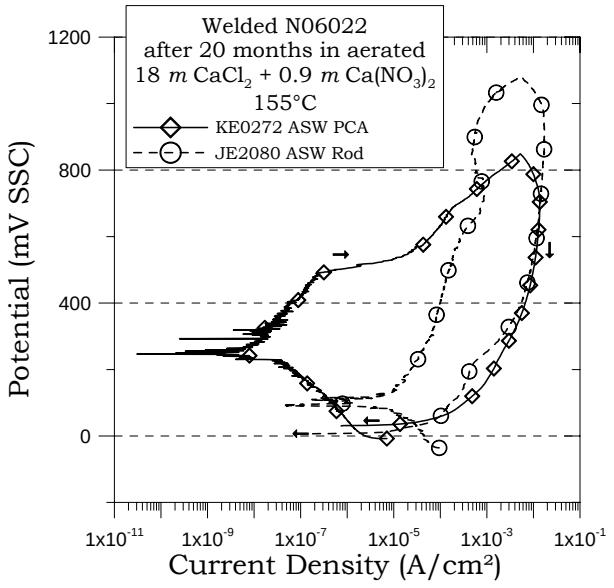

FIGURE 10 – Cyclic Potentiodynamic Polarization for Alloy 22 in 18 *m* $CaCl_2$ + 0.9 *m* $Ca(NO_3)_2$, $[NO_3^-]/[Cl^-]$ = 0.05 at 155°C (Cell 36)

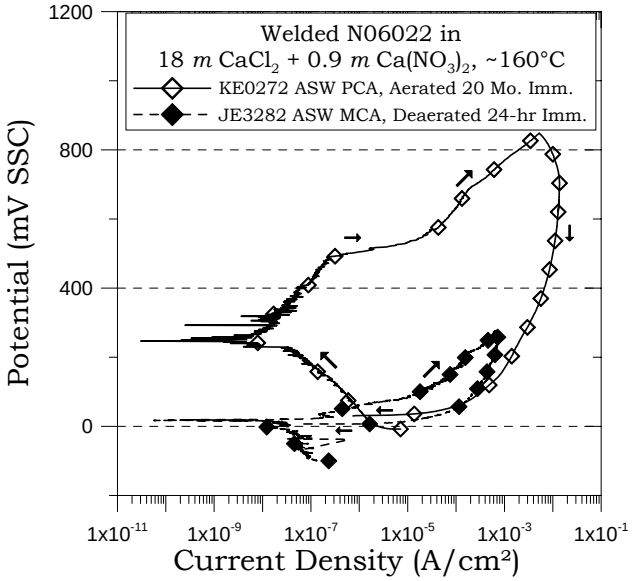

FIGURE 11 – Cyclic Potentiodynamic Polarization for Alloy 22 in 18 *m* $CaCl_2$ + 0.9 *m* $Ca(NO_3)_2$, $[NO_3^-]/[Cl^-]$ = 0.05 at ~ 160°C comparing short and long term immersion. Short term data is at 160°C, long-term at 155°C.

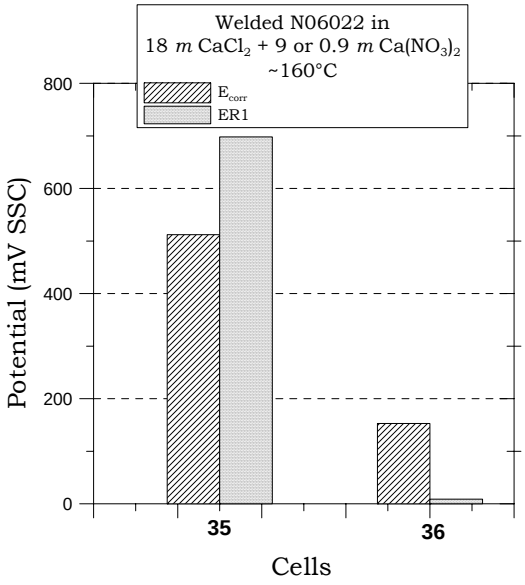

FIGURE 12 – Comparison between E_{corr} and ER1 for Alloy 22 in 18 *m* $CaCl_2$ + 0.9 or 9 *m* $Ca(NO_3)_2$, ~ 160°C. E_{corr} measured at 155°C and ER1 at 160°C. For E_{corr} > ER1, localized corrosion occurred

FIGURE 13 – ASW PCA KE0268 (Front NE) after 20 months immersion in Cell 35.
Original magnification X8

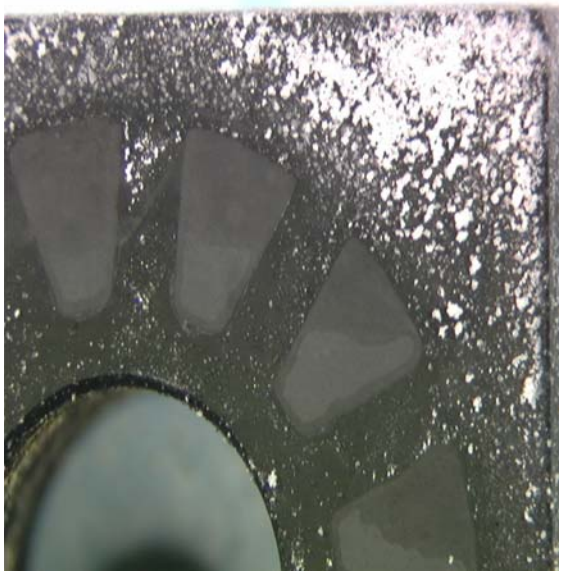

FIGURE 14 – ASW + SHT PCA KE0239 (Front NE) after 20 months immersion in Cell 35.
Original magnification X8

FIGURE 15 – ASW PCA KE0275 (Front NE) after 20 months immersion in Cell 36.
Original magnification X8

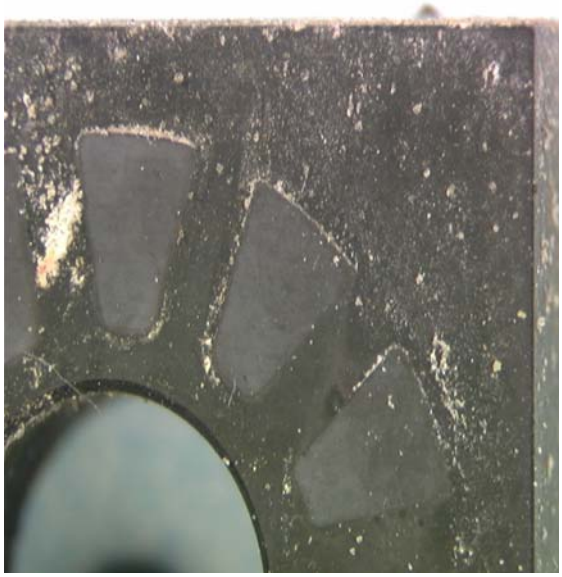

FIGURE 16 – ASW + SHT PCA KE0245 (Front NE) after 20 months immersion in Cell 36.
Original magnification X8